Lipocalin 2 upregulation mediates the detrimental effects of therapy-induced senescence in breast cancer cells.

Jorge Morales-Valencia[1,2,#], Lena Lau[1,#], Ugur Ozerdem[3], Gregory David[1,2,4,*]

[1]Department of Biochemistry and Molecular Pharmacology, NYU Langone Medical Center, New York, NY 10016, USA.
[2]NYU Langone Perlmutter Cancer Center, NYU Langone Health, New York, NY 10016, USA.
[3]Department of Pathology, New York University School of Medicine, NYU Langone Health, New York, NY 10016, USA.
[4]Department of Urology, New York University School of Medicine, NYU Langone Health, New York, NY 10016, USA.
*Address correspondence to Gregory David, Ph. D., gregory.david@nyulangone.org
[#] Contributed equally.

Running title: Senescence-mediated Lipocalin 2 upregulation enhances cancer aggressiveness.

Keywords: Breast Cancer/ Cancer therapy/ Lipocalin 2/ Senescence.

ABSTRACT.

Cancer therapy has improved patient outcomes markedly over the last two decades. However, cancer treatments have been shown to induce senescence in different cell types. Senescent cells secrete a distinct set of factors, collectively termed the senescence-associated secretory phenotype (SASP), which has been postulated to carry both pro- and antitumorigenic properties. Pro-tumorigenic functions of the SASP include enhancement of cancer cell proliferation, induction of epithelial-to-mesenchymal transition and increased migration. The molecular mechanisms by which the SASP regulates these pro-tumorigenic features are poorly understood. Here, we report that exposure to the SASP induces loss of epithelial markers and enhanced migration in breast cancer cells, along with limited transcriptional changes. In particular, we find that Lipocalin 2 (LCN2) is strongly upregulated upon exposure to the SASP, and its inactivation impairs SASP-induced migration. Moreover, we show that in presence of senescence-inducing stimuli, LCN2 promotes breast cancer tumor growth *in vivo*. Finally, we show that neoadjuvant chemotherapy treatment leads to LCN2 upregulation in residual human breast tumors, which correlates with worse overall survival. These findings provide insight into the potential of targeting LCN2 as an adjuvant therapeutic approach to prevent the emergence of aggressive relapsed breast tumors following chemotherapy.

INTRODUCTION.

Breast cancer affects more than one in ten women worldwide (Yedjou, 2019). Currently, neoadjuvant chemotherapy is extensively used to treat breast cancer patients as it helps reduce tumor burden and thus, down staging the disease (Tanaka, 2015). However, most non targeted anticancer agents do not only trigger cytotoxicity in dividing cells, but also engage specific cellular response programs, including senescence, on both cancer cells and the tumor microenvironment (Demaria, 2017).

Cellular senescence refers to the stable cell proliferation arrest caused by either telomere shortening, oncogene activation or genotoxic stress, all of which converge towards the activation of a sustained DNA damage response (DDR) (Rodier, 2011). Because of its engagement in preneoplastic lesions, senescence had been hypothesized to serve as a barrier to malignant transformation, by preventing the proliferation of cells with altered genetic content (Robles, 1998). Conversely, senescent cells accumulate over time in mammals, and directly contribute to the health defects associated with aging (van Deursen, 2014; Childs, 2015), consistent with the theory of antagonistic pleiotropy of senescence (Campisi, 2013). One of the hallmarks of senescence that could explain these otherwise contradictory features is the senescence-associated secretory phenotype (SASP) (Campisi, 2011). The SASP consists of a discrete set of pro-inflammatory cytokines, chemokines and growth factors secreted by senescent cells, in a cellular and senescence inducer-specific manner. Secretion of the SASP results in a pro-inflammatory environment, which resembles features of aging. In addition to its detrimental impact on aging, exposure to the SASP has been reported to promote aggressive traits in tumor models, including increased proliferation (Krtolica, 2001), enhanced angiogenesis (Coppé, 2006) and activation of the epithelial-to-mesenchymal transition (EMT) (Laberge, 2012). However, because the main components of the SASP include a plethora of soluble signaling factors, the molecular mechanisms engaged by senescent cells to drive tumorigenesis remain poorly understood.

Lipocalin 2 (LCN2), also referred to as neutrophil gelatinase-associated lipocalin (NGAL), is a 25 k-Da secreted glycoprotein. LCN2 protein expression levels have been demonstrated to be increased in various cancer types including breast (Yang, 2009; Shi, 2018) colon (Birkenkamp-Demtroder, 2002) and pancreatic (Tong, 2008). Accordingly,

high LCN2 expression has been detected in carcinoma tissues, sera and urine of breast cancer patients (Hu, 2018). Here, we demonstrate that upon exposure to the SASP from senescent cells, breast cancer cells upregulate LCN2, which correlates with an increase in migration and loss of epithelial markers. *In vivo* studies reveal that in presence of senescence-inducing stimuli, LCN2 promotes breast cancer tumor progression. Additionally, we demonstrate that neoadjuvant chemotherapeutic treatment results in LCN2 upregulation in the residual breast tumors in patients, correlating with a decreased expression of epithelial markers and worse prognosis.

RESULTS.

The IL-1-dependent SASP induces features of EMT in MCF7 cells.

We have previously demonstrated that inactivation of the IL-1 pathway can be used to uncouple SASP production from senescence-associated cell cycle exit (Lau, 2019). We leveraged this property of IL-1α inactivated cells to determine the specific pro-tumorigenic effect of the IL-1-dependent SASP. MCF7 breast cancer cells were exposed to conditioned media (CM) from wild-type (WT) TERT-immortalized IMR90 (IMR90T) fibroblasts, senescent WT IMR90Ts (through ectopic expression of oncogenic Ras^{G12V}) and senescent IL-1$\alpha^{-/-}$ IMR90Ts (Figure 1A). We tested the ability of the IL-1-dependent secretome to induce migration in MCF7 cells using a scratch assay. MCF7 cells exposed to CM from senescent WT cells (RasCM) migrated significantly faster than cells exposed to CM from growing cells (Figure 1B, C). Strikingly, CM collected from senescence IL-1$\alpha^{-/-}$ cells was unable to promote cancer cell migration (Figure 1B, C). These observations suggest that exposure to the IL-1α-dependent SASP is sufficient to stimulate breast cancer cells migration. To determine whether SASP-induced increased migration correlates with enhanced chemotactic capacities, MCF7 cells cultured with CM for 2 days were transferred to transwells and allowed to migrate through pores for 48 hours. Consistent with the scratch assay results, MCF7 cells cultured with Ras CM displayed increased migration compared to cells cultured with growing CM or cells cultured with CM from IL-1$\alpha^{-/-}$ cells (Figure 1D). Consistent with our previous demonstration that SASP-production is dependent on the IL-1α/IL-1R axis, senescent CM-induced chemotactic based migration was significantly reduced with CM from senescent IMR90Ts depleted for

the IL-1 receptor (Figure 1E). Furthermore, exposure to senescent CM impacted the morphology of MCF-7 cells, which then adopted a more elongated and fibroblast-like appearance, a feature of EMT (Lamouille, 2014). By contrast, MCF7 cells treated with CM from senescent IL-1$\alpha^{-/-}$ cells maintain their cobblestone-like morphology and strong cell-cell adhesions (Figure 1F). Consistent with these observations, MCF7 cells exposed to senescent CM exhibited a loss of expression of the epithelial marker, E-cadherin (Figure 1G). Finally, the proportion of MCF7 cells expressing the EMT-associated surface marker CD44 (Xu, 2015) increased upon exposure to SASP (Figure 1H). Taken together, these results suggest that exposure to the IL-1-dependent SASP induces features of EMT in MCF7 breast cancer cells.

Exposure to IL-1-dependent SASP induces expression of LCN2 in breast cancer cells.

To begin to understand the molecular mechanism underlying the impact of exposure to the SASP on breast cancer cells' properties, we profiled the transcriptome of MCF7 cells exposed to CM from growing or Ras-induced senescent IMR90Ts. Using a $\log_2$ fold change cutoff 1 and an adjusted p-value of < 0.05, we found 1981 differentially expressed genes between MCF7 cells exposed to growing CM and MCF7 exposed to senescent CM. Gene Ontology analysis indicated that pathways upregulated in senescent CM samples include inflammatory response and extracellular matrix organization (Figure 2A). Additionally, gene set enrichment analysis (GSEA) showed that gene sets that were significantly enriched in senescent CM compared to growing CM samples included Epithelial to Mesenchymal Transition and Protein Secretion (Figure 2B). These results are consistent with previous observations by us and others indicating that exposure to the SASP activates an inflammatory response and transcriptional programs engaged in EMT (Canino, 2012; Ortiz-Montero, 2017). The most upregulated transcript in MCF7 exposed to senescent CM encodes the protein lipocalin-2 (LCN2, or NGAL) (Figure 2C). We confirmed the upregulation of LCN2 mRNA and protein levels via qRT-PCR (Figure 2D) and Western Blot (Figure 2E). LCN2 was not upregulated in MCF7 cells treated with CM from senescent IL-1$\alpha^{-/-}$ cells (Figure 2D, E). To ensure that LCN2 upregulation was independent of the stimulus used to induce senescence, we exposed MCF7 cells to CM

from etoposide (Etop)-treated senescent cells. As for SASP collected from oncogene-induced senescent cells, exposure to SASP from genotoxic-induced senescent cells led to a significant increase in LCN2 mRNA levels (Figure 2F), correlating with the ability of CM from etoposide-induced senescent cells to induce migration in MCF7 cells (Figure 2G). The IL-1dependent SASP also induced expression of LCN2 in SKBR3, Hs578t, BT474, MDAMB231 and T47D breast cancer cells (Figure 2H), showing that LCN2 upregulation upon exposure to conditioned media from senescent cells is independent of ER, PR or HER2 status of breast cancer cells. These cells also exhibited a more elongated and mesenchymal-like morphology upon exposure to senescent CM (data not shown). In addition, we observed an increase in the rate of migration of T47D cells treated with WT Ras CM compared to WT Grow CM after 2 days, albeit at slower rates than MCF7 cells (Figure 2I). Taken all together, these results indicate that the IL-1-dependent SASP secreted from cells induced to senesce by various stimuli promotes migration and LCN2 upregulation in several breast cancer cell lines.

LCN2 upregulation is required for SASP-dependent increased migration in MCF7 cells.

Previous studies have suggested that LCN2 promotes breast cancer progression by enhancing migratory and invasive capabilities of breast cancer cells (Yang, 2009). Because of the substantial LCN2 upregulation observed in cells treated with senescent CM, we hypothesized that the SASP enhances aggressive breast cancer phenotypes at least in part through upregulation of LCN2. To test this, we inactivated LCN2 in MCF7 cells by CRISPR/Cas9 induced gene deletion. Western Blot analysis of MCF7 cells confirmed genetic inactivation of LCN2 upon exposure to CM from growing or senescent cells (Figure 3A, B). In agreement with the undetectable to low levels of LCN2 found in MCF7 cells grown in normal conditions, $LCN2^{-/-}$ MCF7 cells did not exhibit any proliferation defects (data not shown). Strikingly, scratch assays indicated that the SASP-induced increase in migration in MCF7 was largely dependent on the presence of LCN2. $LCN2^{+/+}$ MCF7 cells exposed to senescent CM showed increased migration, closing the gap left by the scratch almost entirely after 3 days in culture, whereas incubation with senescent CM did not result in increased migration in $LCN2^{-/-}$ MCF7 cells (Figure 3C, D).

We also tested the migration capabilities of LCN2 KO cells via transwell assay. Consistent with the scratch assay results, MCF7 LCN2$^{-/-}$ cells cultured with Ras CM displayed decreased migration compared to LCN2$^{+/+}$ (Figure E). Collectively, these results indicate that LCN2 is required for SASP-induced migration of breast cancer cells.

LCN2 potentiates the engagement of an EMT-associated expression program following exposure to senescent conditioned media.

To determine the transcriptional programs engaged by LCN2 in breast cancer cells incubated with senescent CM, RNAseq was performed on LCN2$^{+/+}$ and LCN2$^{-/-}$ MCF7 cells exposed to senescent CM. Using a $\log_2$ fold change cutoff 1 and an adjusted p-value < 0.05, we confirmed LCN2 as one of the most differentially expressed genes (Figure 4A). GSEA revealed differentially enriched genes sets in wild type versus LCN2$^{-/-}$ cells, including “KRas signaling” and “Epithelial to Mesenchymal Transition”. Notably, transcripts related to processes such as “Hypoxia” and “TGFβ signaling” were enriched in LCN2$^{-/-}$ compared to their wild-type counterparts, but their significance is unclear at this point (Figure 4B, C). EMT genes, including CXCL6, CXCL8, were upregulated in MCF7 cells exposed to senescent CM in a LCN2-dependent manner (Figure 4D). Notably, expression of these genes is associated with an early cancer relapse and poor prognosis (Liu, 2019; Shen, 2017). Genes involved in KRas signaling and upregulated in the LCN2$^{+/+}$ cells included CCNA1, NR4A2 and IGFBP2 (Figure 4E). Signaling from the epidermal growth factor receptor (EGFR) plays a pivotal role in tumor progression via proliferation, migration, and survival (Caldieri, 2018). LCN2 has been shown to enhance EGFR cell surface abundance by facilitating its endosomal-mediated recycling (Yammine, 2019). Accordingly, exposing MCF7 cells to senescent CM, resulted in an upregulation of both LCN2 and EGFR in WT cells, whereas LCN2 inactivation was accompanied by a downregulation of EGFR protein levels (Figure 4F). Together, these results suggest that LCN2 upregulation upon exposure to pro-senescence stimuli promotes an increase in EGFR levels and the engagement of an EMT-associated gene expression program.

LCN2 expression and the SASP promote breast cancer tumor progression *in vivo*.

We next sought to assess the impact of LCN2 expression on tumor progression *in vivo*. We injected Luciferase-expressing MDAMB231 cells into mammary fat pads of nude mice and followed tumor progression. When injected alone, MDAMB231 tumors showed similar size 3 weeks post injection regardless of LCN2 status (Figure 5A, B). This indicates that in the absence of a pro-senescence stimulus, LCN2 expression levels remain low (Figure 2H) and hence LCN2 does not have an impact on tumor progression. Western Blot analysis revealed that LCN2 protein levels were reduced significantly only a couple of days after removal of conditioned media from senescent fibroblasts (Figure 5C). Therefore, we opted for a co injection model to support LCN2 expression. Additionally, senescent human fibroblasts have been shown to promote proliferation and tumorigenesis of mutant epithelial cells (Krtolica, 2001). Luminescence analysis revealed that when cultured with senescent fibroblasts, LCN2 promotes proliferation and tumorigenesis of MDAMB231 cells (Figure 5D, E). To further validate our findings, we employed a chemotherapy-induced senescence model. A single dose of 10 mg/kg of doxorubicin potently and rapidly increases the *in vivo* burden of senescent cells in humans and in mice. Importantly, this senescence induction is accompanied by SASP secretion (De Maria, 2016). We injected Luciferase-expressing MDAMB231 cells into mammary fat pads of nude mice. Once tumors were established, mice were treated with doxorubicin. While $LCN2^{+/+}$ and $LCN2^{-/-}$ tumors grew at a comparable rate, one week after doxorubicin treatment $LCN2^{+/+}$ tumors were significantly larger in size when compared to their $LCN2^{-/-}$ counterparts (Figure 5F, G). These results suggest that senescence-mediated LCN2 expression leads to tumor progression in breast cancer cell-derived xenografts.

LCN2 upregulation following chemotherapy is a poor prognostic factor in breast cancer patients.

To assess the clinical relevance of these observations, we analyzed LCN2 levels in biopsy samples from breast cancer patients collected prior to or following neo-adjuvant chemotherapy treatment. Chemotherapy treated samples displayed increased in positivity for the SASP marker IL-6 (Figure 6A, B). Along IL-6 upregulation, samples

collected after neoadjuvant chemotherapy treatment exhibited increased LCN2 reactivity, while all biopsy samples collected before chemotherapy treatment displayed undetectable or low LCN2 expression (Figure 6A, C). The opposite effect was observed for the epithelial marker, E-cadherin (Figure 6A, D). We further analyzed the correlations between LCN2 levels and prognosis in breast cancer patients using publicly available expression databases. The analysis revealed that LCN2 was upregulated at the mRNA level in 125 of 2,507 patient samples (7%). Patients with increased levels of LCN2 have an inferior overall (Data not shown) and relapse-free survival compared to those with unaltered levels of LCN2 (Figure 6E). Additionally, 52.8% of patients with high LCN2 levels had received chemotherapy treatment prior to analysis, while only 18.5% of the patients with low levels of LCN2 had (Figure 6F), further indicating a correlation between chemotherapy treatment and increased LCN2 levels. This data suggests that LCN2 could be a potential prognostic biomarker for breast cancer.

DISCUSSION.

Therapy-induced senescence (TIS) has emerged as a novel functional target to improve cancer therapy (Ewald, 2010). High-throughput screens have been employed to find drug targets that trigger senescence in cancer cells (Wang, 2017). However, therapy-induced senescence could be detrimental as well and can potentially drive many aspects of cancer progression, as the SASP of senescent cells has been shown to harbor both pro- and anti-tumorigenic properties depending on cell type and context (Lau, 2019). Additionally, evidence shows that there is a link between TIS and stem cell self-renewing features (Sieben, 2018). Recent findings show that a senescence-like population of chemotherapy-resilient cells is capable of initiating recurrence of AML by increasing their stemness potential (Duy, 2021). Indeed, cellular senescence has been shown to induce a transcriptional reprogramming that promotes cancer stemness, resulting in cells with highly aggressive growth potential (Milanovic, 2017).

We report here that SASP exposure induces features of EMT in breast cancer cells. Our results are consistent with previous findings showing that breast cancer cells exposed to the SASP exhibit epithelial cell scattering and reduced cell-cell adhesions (Coppé, 2008). SASP-mediated recruitment of immune cells, such as M2-type macrophages and

myeloid-derived suppressor cells (MDSCs), can create an inflammatory environment that further drives tumorigenesis. Inflammatory factors released by cells undergoing EMT may also contribute to the establishment of this microenvironment or may act in an autocrine manner to reinforce the EMT phenotype (Singh, 2019).

Additionally, we demonstrate that Lipocalin 2 (LCN2) upregulation is required for the engagement of an EMT-associated expression program. Several studies have suggested that LCN2 induction drives EMT and metastasis of breast cancer cells (Shi, 2008; Leng, 2009). However, the mechanism employed by LCN2 to induce EMT remains elusive. Previous studies suggest that downregulation of the estrogen receptor ERα induces expression of the transcription factor Slug, driving LCN2-induced EMT. Our transcriptome analyses indicate that ERα is indeed downregulated and Slug is upregulated in MCF7 cells treated with senescent CM compared to those treated with growing CM (data not shown). Studies have demonstrated that ERα signaling helps maintain the epithelial phenotype through inhibition of Snail activity (Fujita, 2003). LCN2 has also been shown to drive EMT *in vitro* via its interaction with MMP9, reducing E-cadherin expression levels on the cell surface (Xie, 2004). Further experiments will be necessary to elucidate the mechanism employed by LCN2 to promote EMT in breast cancer cells.

Lipocalin-2 (LCN2) was first discovered to impede iron sequestration and inhibit proliferation of Gram-negative bacteria, therefore participating in innate immunity (Goetz, 2002). However, the effect of LCN2 on the tumor microenvironment is far from being fully understood. It was recently shown that cancer cells use LCN2 to outcompete macrophages and support their growth in a model for Leptomeningeal Metastasis (Chi, 2020). Moreover, LCN2 has the ability to induce upregulation of human leukocyte antigen G (HLA-G), the role of HLA-G as a tumor immune escape mechanism has been demonstrated in mouse models (Lin, 2010; Abella, 2015). Therefore, LCN2 inactivation could also be proven beneficial by increasing patients' response to immunotherapy.

Moreover, consistent with observations from other groups, we show here that LCN2 expression leads to tumor progression *in vivo* (Chaudhary, 2021; Huang, 2020, Berger, 2010). Whether senescence-mediated LCN2 upregulation promotes metastasis of breast cancer remains to be elucidated. LCN2 overexpression has been observed in many types of cancer including breast and pancreas (Rodvold, 2012). Besides LCN2 upregulation by

inflammation in the tumor microenvironment, LCN2 has been shown to be upregulated in Systemic lupus erythematosus (SLE) patients (Li, 2014). Additionally, serum concentrations of LCN2 are closely associated with obesity and its related chronic inflammation (Jang, 2012). More studies are necessary to know whether LCN2 is also upregulated with other sources of inflammation such as SARS-Cov-2 infection and aging. This is interesting because with increasing age, the immune system undergoes profound changes as reflected by an inability to clear senescent cells and increased susceptibility to infection and cancer development. LCN2 could represent a target to prevent cancer development in aged patients.

Aside from its effect on the immune response, LCN2 could be impacting tumor cells metabolism. Iron is known to facilitate tumorigenesis by driving cell proliferation (Richardson, 2009). Therefore, LCN2 upregulation could result in an increased ability to sequester iron and regulate it intracellularly. It is known that an increased capacity for iron sequestration in breast cancer cells is associated with aggressive tumor growth (Pinnix, 2010). Iron chelators have been used to slow cancer progression in vivo and iron transport has been recently shown to play a key-role in LCN2-dependent cancer growth (Chi, 2020).

More mechanistic studies into which specific pathways are active in $LCN2^{+/+}$ cells will provide more insight into the potential use of LCN2 as a therapeutic target to be exploited to reduce breast cancer cell aggressiveness. Concurrently, chemical inhibition or iron chelation of LCN2 should be tested to determine its therapeutic targetability in breast cancer, as well as potential off-target effects of this treatment. Additionally, more comprehensive studies exploring the specific effects of the SASP during different cancer stages, as well as in various tissue contexts, will provide important insight into therapeutic targets for more personalized and effective cancer treatment.

MATERIALS AND METHODS.

Cells. IMR90 primary lung embryonic fibroblasts expressing hTERT (IMR90Ts) were obtained from S. Smith (NYU School of Medicine, New York, NY). Cells were cultured in MEM (Corning) supplemented with 10% fetal bovine serum and 1% penicillin-streptomycin (Cellgro). MCF7, SKBR3, Hs578t and T47D cells were obtained from R. Possemato (NYU School of Medicine, New York, NY). MDAMB231 cells were obtained from E. Hernando (NYU School of Medicine, New York, NY). BT474 cells were obtained from B. Neel (NYU School of Medicine, New York, NY). Breast cancer cells (except T47D) were cultured in DMEM (Corning) supplemented with 10% FBS and 1% penicillin/streptomycin. T47D cells were cultured in RPM1 1640 media (Corning) supplemented with 10% FBS and 1% penicillin/streptomycin. Py8119 cells (ATCC) were cultured in F-12K medium (Gibco) supplemented with 10% FBS and 1% penicillin/streptomycin. HEK293T cells (ATCC) were used to generate retro- and lentiviruses and were cultured in DMEM (Corning), supplemented with 10% donor calf serum and 1% penicillin-streptomycin. IMR90T cells were maintained in 6% O_2 and 5% CO_2 at 37°C, while 293T and breast cancer cells were maintained in 5% CO2 at 37°C.

Senescence induction and condition media (CM) harvest. For Ras-induced senescence, IMR90T-Ras-ERT2 were treated with 200 nM tamoxifen (Sigma) continuously for 10 days. Fresh media and tamoxifen were added every 2-3 days. Cells were treated with an equal volume of ethanol as control. On day 8 of Ras induction, media was replaced with serum-free media and harvested after 48 h. For etoposide-induced senescence, cells were treated with 50 uM etoposide (Sigma) or an equal volume of DMSO as a control for 48 hours. Etoposide-containing medium was then replaced by normal culture media for 5 days. 7 days after etoposide treatment, media was replaced with serum-free media and harvested after 48 h. Conditioned media was aliquoted and flash frozen in liquid nitrogen before storing at -80 C.

Scratch assays. MCF7 or T47D cells were grown in 6-well plates until confluent. A P200 tip was used to create vertical scratches. Media was then changed to media containing 1% FBS supplemented by CM from growing or senescent cells. Amount of CM added was normalized to cell number. CM was replaced every day. Pictures of scratches per well were taken each day for 3 days. Using Adobe Photoshop, the gap width was

measured as the number of pixels that comprise the gap. The data is presented as relative gap width compared to gap width of each sample at day 0.

Transwell migration assays. MCF7 cells were exposed to 1-3 mL CM from growing or senescent cells. Fresh CM was added every day for a total of 2 days. Cells were then trypsinized and counted. A total of 50,000 cells in 100 uL serum-free DMEM were seeded on top of transwells containing 8 um pores for use in 24-well plates. 1 mL of DMEM supplemented with 20% FBS was added to the bottom of the wells and cells were allowed to migrate for 48 h. Transwells were then washed in PBS and fixed in 1% glutaraldehyde in PBS for 20 minutes, and crystal violet for 30 min rocking. Values are expressed as fold change in the number of cells compared to the number of cells cultured in the corresponding growing CM.

Immunofluorescence. MCF7 cells were treated with CM from growing or senescent cells. CM was added every day for 2 days. Cells were then plated on coverslips before being fixed in 4% paraformaldehyde (SCBT) for 10 min at RT. Cells were permeabilized with cold 0.1% Triton X-100 in PBS for 5 min and blocked with 20% donkey serum in PBST for 15 min. Cells were incubated with mouse anti-E-cadherin (Millipore, MAB1199) at 1:200 dilution in blocking solution at 37°C for 1 h. Cells were then washed and incubated in Cy3-conjugated donkey anti-mouse IgG (Jackson Immunoresearch) for 1 hour at RT. Cells were mounted with mounting medium containing Dapi (Vectashield). Slides were examined on a Zeiss AxioImager A2 microscope. A total of 100 cells per cover-slip were counted. Amount E-cadherin staining was quantified as number of red pixels per Dapi-positive cells using Image J to calculate pixels.

Transcriptomics analysis. MCF7 cells were cultured in CM from growing or Ras-induced senescent cells for 2 days. MCF7 LCN2$^{+/+}$ and LCN2$^{-/-}$ cells were cultured in CM from Ras-induced senescent cells for 2 days. RNA quality assessment, library preparation and sequencing were performed by the NYU School of Medicine Genome Technology Center or by Genewiz. Strand-specific libraries were prepared using the TruSeq RNA library Prep kit, and libraries were sequenced on an Illumina HiSeq2500 using 50-bp paired-end reads. Sequences were mapped to the hg10 genome, and analysis was done as previously described (Proudhon, 2016).

Real-Time PCR. Total RNA was extracted using TRIzol (Life Technologies) according to manufacturer's instructions. 1 ug of total RNA was used to generate cDNA with oligo dT. Real-time qPCR was performed using Maxima SYBR Green (Fisher Scientific) and samples were run on a Bio-Rad Cycler MyiQ. The following sets of primer were used: *hTubulin* forward 5'-cttcgtctccgccatcag-3', reverse 5'-ttgccaatctggacacca-3', *hLCN2* forward 5'-gaagtctgactactggatcagga-3', reverse 5'-accactcggacgaggtaact-3', *mGAPDH* forward 5'-cacggcaaattcaacggcacagtc-3', reverse 5'-acccgtttggctccacccttca-3', *mLCN2* forward 5'-gacttccggagcgatcagtt-3', reverse 5'-ttctgatccagtagcgacagc-3'.

CRISPR/Cas 9 editing. sgRNAs were cloned into lentiCRISPR v2 (Addgene) and 48 hours after infection, cells were selected with puromycin (1 ug/mL) for at least 4 days before plating single cell clones. The following sgRNA's were used for hLCN2: forward 5'-caccgaagtggtatgtggtag-3', reverse 5'-aaacggcctaccacataccacttc-3' and forward 5'-caccgtggtggcatacatctt-3', reverse 5'-aaacgcaaaagatgtatgccacca-3'.

Protein extraction and Western blotting. Cells were lysed in 1× RIPA buffer (1% NP-40, 0.1% SDS, 50 mM Tris-HCl, pH 7.4, 150 mM NaCl, 0.5% sodium deoxycholate, 1 mM EDTA), 0.5 μM DTT, 25 mM NaF, 1 mM sodium vanadate, 1 mM PMSF, and cOmplete protease cocktail inhibitor (Sigma). Samples were resolved by SDS-PAGE and analyzed by standard western blotting techniques. The following primary antibodies were used: mouse anti-tubulin (Sigma T9026) at 1:2000 dilution, goat anti-LCN2 (R&D AF1747) at 0.2 ug/mL, mouse anti-vinculin (Sigma V9131) at 1:1000 dilution and rabbit anti-EGFR (Cell Signaling 4267) at 1:1000 dilution.

MDAMB231 co-injection with senescent fibroblasts. 2.5×10^5 $LCN2^{+/+}$ or $LCN2^{-/-}$ MDAMB231 GFP-Luciferase cells were pretreated with RasCM for 48 hours before being injected into the inguinal mammary fat pad of 4-6 weeks old female nude mice with 1×10^6 senescent IMR90T cells in 50% Matrigel (Corning).

MDAMB231 doxorubicin-induced senescence model. 1×10^5 $LCN2^{+/+}$ or $LCN2^{-/-}$ MDAMB231 GFP-Luciferase cells in 50% Matrigel (Corning) were injected into the inguinal mammary fat pad of 4-6 weeks old female nude mice. Once tumors were established, mice were treated with a single dose of 10 mg/kg of doxorubicin (Sigma).

Bioluminescence. For in vivo luminescence of Luciferase, mice were injected i.p. with of 150 mg of D-Luciferin (ThermoFisher) per kg of body weight. Fifteen minutes later, the

mice were anesthetized with isoflurane and luminescence was measured with a PerkinElmer IVIS Spectrum system.

Immunohistochemical staining. Immunohistochemical staining was performed at the NYU Langone Experimental Pathology Research Laboratory as previously described (Rielland, 2014). The following antibodies were used: goat anti-LCN2 (R&D AF1747), E-cadherin (Cell Signal, 3195T), IL-6 (Santa Cruz Biotechnology, sc-1265).

Statistical Analysis. Results were analyzed using GraphPad Prism software. Values were subjected to unpaired two-tailed t-tests, multiple t-tests, one-way ANOVA followed by Dunnett's multiple comparisons test, or two-way ANOVA followed by Tukey's multiple comparisons test. Data is presented as means ± SEM.

ACKNOWLEDGEMENTS

The authors sincerely thank all members of the David lab for helpful discussions during the preparation of this manuscript. We wish to acknowledge the NYU Genome Technology Center for help with RNA sequencing (RNA-seq). We thank Dr. Richard Possemato (NYU School of Medicine), Dr. Eva Hernando (NYU School of Medicine), Dr. Benjamin Neel (NYU School of Medicine) and Dr. Judith Campisi (Buck Institute for Research on Aging) as well as members of their labs for the generous gift or reagents and plasmids and for helpful discussions. This work was funded by NIH/NCI (CA246416) [GD], NYS DoH (C36617GG) [GD] and the NYSTEM Institutional Training Grant (C322560GG) [JMV].

AUTHOR CONTRIBUTIONS

JMV and LL designed and performed the experiments presented in this manuscript and analyzed the data. UD provided patient samples and analyzed the data. GD designed the study and supervised the research. JMV and GD wrote the manuscript.

CONFLICT OF INTEREST

The authors declare no competing interests.

REFERENCES.

1. Abella, V., Scotece, M., Conde, J., Gómez, R., Lois, A., Pino, J., Gómez-Reino, J. J., Lago, F., Mobasheri, A., & Gualillo, O. (2015). The potential of lipocalin-2/NGAL as biomarker for inflammatory and metabolic diseases. Biomarkers: biochemical indicators of exposure, response, and susceptibility to chemicals, 20(8), 565–571.
2. Berger T, Cheung CC, Elia AJ, Mak TW. (2010). Disruption of the Lcn2 gene in mice suppresses primary mammary tumor formation but does not decrease lung metastasis. Proc Natl Acad Sci U S A, 107(7):2995-3000.
3. Birkenkamp-Demtroder K, Christensen LL, Olesen SH, Frederiksen CM, Laiho P, Aaltonen LA, Laurberg S, Sørensen FB, Hagemann R, ØRntoft TF. (2002). Gene expression in colorectal cancer. Cancer Research, 62(15):4352-63.
4. Caldieri G, Malabarba MG, Di Fiore PP, Sigismund S. (2018). EGFR Trafficking in Physiology and Cancer. Progress in Molecular and Subcellular Biololy, 57:235-272.
5. Campisi, J., Andersen, J. K., Kapahi, P., & Melov, S. (2011). Cellular senescence: a link between cancer and age-related degenerative disease? Seminars in cancer biology, 21(6), 354–359.
6. Campisi J. (2013). Aging, cellular senescence, and cancer. Annual review of physiology, 75, 685–705.
7. Canino, C., Mori, F., Cambria, A., Diamantini, A., Germoni, S., Alessandrini, G., Borsellino, G., Galati, R., Battistini, L., Blandino, R., Facciolo, F., Citro, G., Strano, S., Muti, P., Blandino, G., & Cioce, M. (2012). SASP mediates chemoresistance and tumor-initiating-activity of mesothelioma cells. Oncogene, 31(26), 3148–3163.
8. Chaffer, C. L., & Weinberg, R. A. (2011). A perspective on cancer cell metastasis. Science (New York, N.Y.), 331(6024), 1559–1564.
9. Chaudhary N, Choudhary BS, Shah SG, Khapare N, Dwivedi N, Gaikwad A, Joshi N, Raichanna J, Basu S, Gurjar M, P K S, Saklani A, Gera P, Ramadwar M, Patil P, Thorat R, Gota V, Dhar SK, Gupta S, Das M, Dalal SN. (2021). Lipocalin 2 expression promotes tumor progression and therapy resistance by inhibiting

ferroptosis in colorectal cancer. International Journal of Cancer, 149(7):1495-1511.

10. Chi, Y., Remsik, J., Kiseliovas, V., Derderian, C., Sener, U., Alghader, M., Saadeh, F., Nikishina, K., Bale, T., Iacobuzio-Donahue, C., Thomas, T., Pe'er, D., Mazutis, L., & Boire, A. (2020). Cancer cells deploy lipocalin-2 to collect limiting iron in leptomeningeal metastasis. Science (New York, N.Y.), 369(6501), 276–282.
11. Childs, B. G., Durik, M., Baker, D. J., & van Deursen, J. M. (2015). Cellular senescence in aging and age-related disease: from mechanisms to therapy. Nature medicine, 21(12), 1424–1435.
12. Coppé, J. P., Kauser, K., Campisi, J., & Beauséjour, C. M. (2006). Secretion of vascular endothelial growth factor by primary human fibroblasts at senescence. The Journal of biological chemistry, 281(40), 29568–29574.
13. Coppé, J. P., Patil, C. K., Rodier, F., Sun, Y., Muñoz, D. P., Goldstein, J., Nelson, P. S., Desprez, P. Y., & Campisi, J. (2008). Senescence-associated secretory phenotypes reveal cell-nonautonomous functions of oncogenic RAS and the p53 tumor suppressor. PLoS biology, 6(12), 2853–2868.
14. Cuollo, L., Antonangeli, F., Santoni, A., & Soriani, A. (2020). The Senescence-Associated Secretory Phenotype (SASP) in the Challenging Future of Cancer Therapy and Age-Related Diseases. Biology, 9(12), 485.
15. Demaria, M., O'Leary, M. N., Chang, J., Shao, L., Liu, S., Alimirah, F., Koenig, K., Le, C., Mitin, N., Deal, A. M., Alston, S., Academia, E. C., Kilmarx, S., Valdovinos, A., Wang, B., de Bruin, A., Kennedy, B. K., Melov, S., Zhou, D., Sharpless, N. E., … Campisi, J. (2017). Cellular Senescence Promotes Adverse Effects of Chemotherapy and Cancer Relapse. Cancer discovery, 7(2), 165–176.
16. Duy, C., Li, M., Teater, M., Meydan, C., Garrett-Bakelman, F. E., Lee, T. C., Chin, C. R., Durmaz, C., Kawabata, K. C., Dhimolea, E., Mitsiades, C. S., Doehner, H., D'Andrea, R. J., Becker, M. W., Paietta, E. M., Mason, C. E., Carroll, M., & Melnick, A. M. (2021). Chemotherapy induces senescence-like resilient cells capable of initiating AML recurrence. Cancer discovery, candisc.1375.2020.

17. Ewald, J. A., Desotelle, J. A., Wilding, G., & Jarrard, D. F. (2010). Therapy-induced senescence in cancer. Journal of the National Cancer Institute, 102(20), 1536–1546.
18. Fujita, N., Jaye, D. L., Kajita, M., Geigerman, C., Moreno, C. S., & Wade, P. A. (2003). MTA3, a Mi-2/NuRD complex subunit, regulates an invasive growth pathway in breast cancer. Cell, 113(2), 207–219.
19. Goetz, D. H., Holmes, M. A., Borregaard, N., Bluhm, M. E., Raymond, K. N., & Strong, R. K. (2002). The neutrophil lipocalin NGAL is a bacteriostatic agent that interferes with siderophore-mediated iron acquisition. Molecular cell, 10(5), 1033–1043.
20. Huang T, Li Y, Zhou Y, Lu B, Zhang Y, Tang D, Gan Y, He Z, Chen Z, Yu W, Li P. (2020). Stroke Exacerbates Cancer Progression by Upregulating LCN2 in PMN-MDSC. Frontiers in Immunology,11:299.
21. Hu C, Yang K, Li M, Huang W, Zhang F, Wang H. (2018). Lipocalin 2: a potential therapeutic target for breast cancer metastasis. OncoTargets and Therapy, 11:8099-8106.
22. Jang, Y., Lee, J. H., Wang, Y., & Sweeney, G. (2012). Emerging clinical and experimental evidence for the role of lipocalin-2 in metabolic syndrome. Clinical and experimental pharmacology & physiology, 39(2), 194–199.
23. Krtolica, A., Parrinello, S., Lockett, S., Desprez, P. Y., & Campisi, J. (2001). Senescent fibroblasts promote epithelial cell growth and tumorigenesis: a link between cancer and aging. Proceedings of the National Academy of Sciences of the United States of America, 98(21), 12072–12077.
24. Laberge, R. M., Awad, P., Campisi, J., & Desprez, P. Y. (2012). Epithelial-mesenchymal transition induced by senescent fibroblasts. Cancer microenvironment: official journal of the International Cancer Microenvironment Society, 5(1), 39–44.
25. Lamouille, S., Xu, J., & Derynck, R. (2014). Molecular mechanisms of epithelial-mesenchymal transition. Nature reviews. Molecular cell biology, 15(3), 178–196.

26. Lau, L., & David, G. (2019). Pro- and anti-tumorigenic functions of the senescence-associated secretory phenotype. Expert opinion on therapeutic targets, 23(12), 1041–1051.
27. Lau, L., Porciuncula, A., Yu, A., Iwakura, Y., & David, G. (2019). Uncoupling the Senescence-Associated Secretory Phenotype from Cell Cycle Exit via Interleukin-1 Inactivation Unveils Its Protumorigenic Role. Molecular and cellular biology, 39(12), e00586-18.
28. Leng, X., Ding, T., Lin, H., Wang, Y., Hu, L., Hu, J., Feig, B., Zhang, W., Pusztai, L., Symmans, W. F., Wu, Y., & Arlinghaus, R. B. (2009). Inhibition of lipocalin 2 impairs breast tumorigenesis and metastasis. Cancer research, 69(22), 8579–8584.
29. Li, Y. N., Hu, F. L., Dai, Y. J., Li, R., Ma, X. X., Du, Y., Feng, M., Jia, Y., Zhang, C. F., Zhu, L., Ascherman, D. P., & Li, Z. G. (2014). Serum anti-lipocalin 2 IgG is a novel biomarker in the diagnosis of systemic lupus erythematosus. Lupus, 23(9), 868–875.
30. Lin, A., Zhang, X., Xu, H. H., Xu, D. P., Ruan, Y. Y., & Yan, W. H. (2012). HLA-G expression is associated with metastasis and poor survival in the Balb/c nu/nu murine tumor model with ovarian cancer. International journal of cancer, 131(1), 150–157.
31. Liu, G., An, L., Zhang, H., Du, P., & Sheng, Y. (2019). Activation of CXCL6/CXCR1/2 Axis Promotes the Growth and Metastasis of Osteosarcoma Cells in vitro and in vivo. Frontiers in pharmacology, 10, 307.
32. Milanovic, M., Fan, D., Belenki, D., Däbritz, J., Zhao, Z., Yu, Y., Dörr, J. R., Dimitrova, L., Lenze, D., Monteiro Barbosa, I. A., Mendoza-Parra, M. A., Kanashova, T., Metzner, M., Pardon, K., Reimann, M., Trumpp, A., Dörken, B., Zuber, J., Gronemeyer, H., Hummel, M., … Schmitt, C. A. (2018). Senescence-associated reprogramming promotes cancer stemness. Nature, 553(7686), 96–100.
33. Ortiz-Montero, P., Londoño-Vallejo, A., & Vernot, J. P. (2017). Senescence-associated IL-6 and IL-8 cytokines induce a self- and cross-reinforced

senescence/inflammatory milieu strengthening tumorigenic capabilities in the MCF-7 breast cancer cell line. Cell communication and signaling: CCS, 15(1), 17.

34. Pinnix, Z. K., Miller, L. D., Wang, W., D'Agostino, R., Jr, Kute, T., Willingham, M. C., Hatcher, H., Tesfay, L., Sui, G., Di, X., Torti, S. V., & Torti, F. M. (2010). Ferroportin and iron regulation in breast cancer progression and prognosis. Science translational medicine, 2(43), 43ra56.
35. Proudhon, C., Snetkova, V., Raviram, R., Lobry, C., Badri, S., Jiang, T., Hao, B., Trimarchi, T., Kluger, Y., Aifantis, I., Bonneau, R., & Skok, J. A. (2016). Active and Inactive Enhancers Cooperate to Exert Localized and Long-Range Control of Gene Regulation. Cell reports, 15(10), 2159–2169.
36. Rielland, M., Cantor, D. J., Graveline, R., Hajdu, C., Mara, L., Diaz, B., Miller, G., & David, G. (2014). Senescence-associated SIN3B promotes inflammation and pancreatic cancer progression. The Journal of clinical investigation, 124(5), 2125–2135.
37. Robles, S. J., & Adami, G. R. (1998). Agents that cause DNA double strand breaks lead to p16INK4a enrichment and the premature senescence of normal fibroblasts. Oncogene, 16(9), 1113–1123.
38. Rodier, F., & Campisi, J. (2011). Four faces of cellular senescence. The Journal of cell biology, 192(4), 547–556.
39. Rodvold JJ, Mahadevan NR, Zanetti M. (2012). Lipocalin 2 in cancer: when good immunity goes bad. Cancer Letters, 316(2):132-8.
40. Sieben, C. J., Sturmlechner, I., van de Sluis, B., & van Deursen, J. M. (2018). Two-Step Senescence-Focused Cancer Therapies. Trends in cell biology, 28(9), 723–737.
41. Shen, T., Yang, Z., Cheng, X., Xiao, Y., Yu, K., Cai, X., Xia, C., & Li, Y. (2017). CXCL8 induces epithelial-mesenchymal transition in colon cancer cells via the PI3K/Akt/NF-κB signaling pathway. Oncology reports, 37(4), 2095–2100.
42. Shi, H., Gu, Y., Yang, J., Xu, L., Mi, W., & Yu, W. (2008). Lipocalin 2 promotes lung metastasis of murine breast cancer cells. Journal of experimental & clinical cancer research: CR, 27(1), 83.

43. Singh, S., & Chakrabarti, R. (2019). Consequences of EMT-Driven Changes in the Immune Microenvironment of Breast Cancer and Therapeutic Response of Cancer Cells. Journal of clinical medicine, 8(5), 642.
44. Tanaka, S., Iwamoto, M., Kimura, K., Matsunami, N., Morishima, H., Yoshidome, K., Nomura, T., Morimoto, T., Yamamoto, D., Tsubota, Y., Kobayashi, T., & Uchiyama, K. (2015). Phase II Study of Neoadjuvant Anthracycline-Based Regimens Combined With Nanoparticle Albumin-Bound Paclitaxel and Trastuzumab for Human Epidermal Growth Factor Receptor 2-Positive Operable Breast Cancer. Clinical breast cancer, 15(3), 191–196.
45. Thiery, J. P., Acloque, H., Huang, R. Y., & Nieto, M. A. (2009). Epithelial-mesenchymal transitions in development and disease. Cell, 139(5), 871–890.
46. Tong Z, Kunnumakkara AB, Wang H, Matsuo Y, Diagaradjane P, Harikumar KB, Ramachandran V, Sung B, Chakraborty A, Bresalier RS, Logsdon C, Aggarwal BB, Krishnan S, Guha S. (2008). Neutrophil gelatinase-associated lipocalin: a novel suppressor of invasion and angiogenesis in pancreatic cancer. Cancer Research, 68(15):6100-8.
47. van Deursen J. M. (2014). The role of senescent cells in ageing. Nature, 509(7501), 439–446.
48. Wang, L., Leite de Oliveira, R., Wang, C., Fernandes Neto, J. M., Mainardi, S., Evers, B., Lieftink, C., Morris, B., Jochems, F., Willemsen, L., Beijersbergen, R. L., & Bernards, R. (2017). High-Throughput Functional Genetic and Compound Screens Identify Targets for Senescence Induction in Cancer. Cell reports, 21(3), 773–783.
49. Xie, L., Law, B. K., Chytil, A. M., Brown, K. A., Aakre, M. E., & Moses, H. L. (2004). Activation of the Erk pathway is required for TGF-beta1-induced EMT in vitro. Neoplasia (New York, N.Y.), 6(5), 603–610.
50. Xu, H., Tian, Y., Yuan, X., Wu, H., Liu, Q., Pestell, R. G., & Wu, K. (2015). The role of CD44 in epithelial-mesenchymal transition and cancer development. OncoTargets and Therapy, 8, 3783–3792.

51. Yammine, L., Zablocki, A., Baron, W., Terzi, F., & Gallazzini, M. (2019). Lipocalin-2 Regulates Epidermal Growth Factor Receptor Intracellular Trafficking. Cell reports, 29(7), 2067–2077.
52. Yang, J., Bielenberg, D. R., Rodig, S. J., Doiron, R., Clifton, M. C., Kung, A. L., Strong, R. K., Zurakowski, D., & Moses, M. A. (2009). Lipocalin 2 promotes breast cancer progression. Proceedings of the National Academy of Sciences of the United States of America, 106(10), 3913–3918.
53. Yang J, Moses MA. (2009). Lipocalin 2: a multifaceted modulator of human cancer. Cell Cycle, 8(15):2347-52.
54. Yedjou, C. G., Sims, J. N., Miele, L., Noubissi, F., Lowe, L., Fonseca, D. D., Alo, R. A., Payton, M., & Tchounwou, P. B. (2019). Health and Racial Disparity in Breast Cancer. Advances in experimental medicine and biology, 1152, 31–49.

FIGURES.

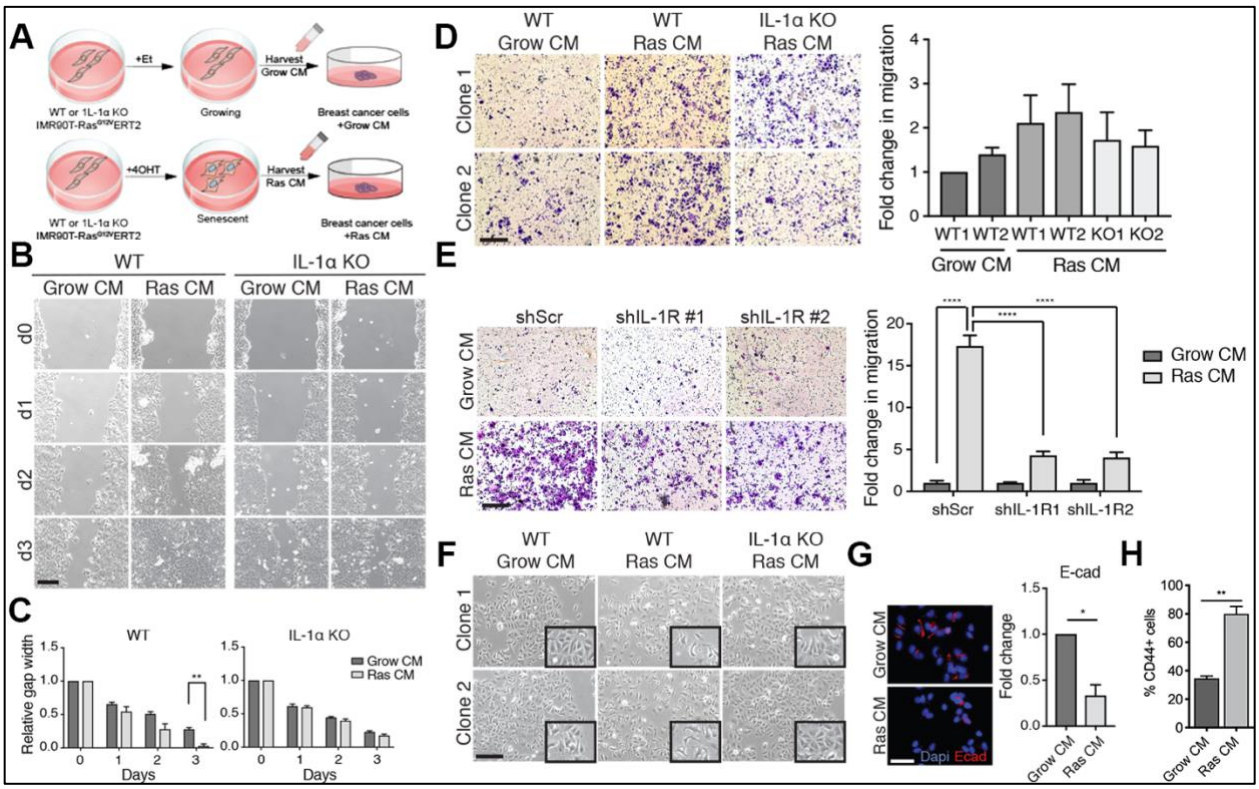

Figure 1. The IL-1-dependent SASP promotes migration of breast cancer cells. (A) MCF7 breast cancer cells were exposed to conditioned media (CM) from wild-type (WT) TERT-immortalized IMR90 (IMR90T) fibroblasts, senescent WT IMR90Ts (through ectopic expression of oncogenic Ras, Ras^{V12}) and senescent IL-1$\alpha^{-/-}$ IMR90Ts (B) Representative images of scratched MCF7 cells cultured in conditioned media (CM) from growing (Grow CM) or Ras-senescent (Ras CM) IMR90T cells with or without IL-1α for 3 days. Scale bar = 200 um (C) Quantification of relative gap width of MCF7 cultures treated with the indicated CM. (D, E) Representative images and quantification of transwell migration assays of MCF7 cells treated with the indicated CM. (F) Representative images of MCF7 cells treated with CM from 1 of 2 IMR90T clones, either growing or Ras-induced senescent with or without IL-1α . Inset: magnified images. Scale bar = 200 um. (G) Representative images and quantification of E-cadherin immunofluorescence staining in MCF7 cells treated with the indicated CM. Scale bar = 50 um. (H) Quantification of CD44^{+} MCF7 cells after being treated with the indicated CM as analyzed by flow cytometry. n = 3, * $p < 0.05$.

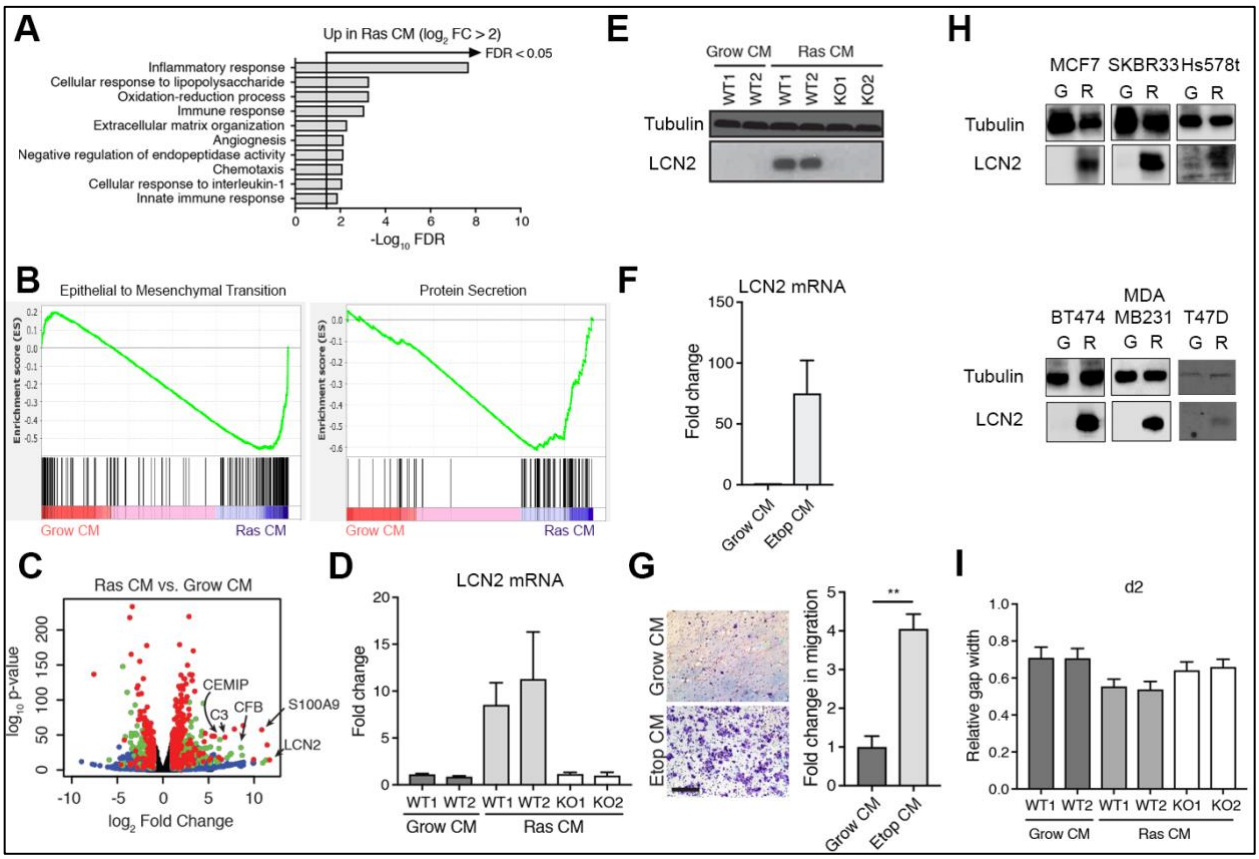

Figure 2. Exposure to IL-1-dependent SASP induces expression of LCN2 in breast cancer cells. (A) Gene ontology analysis of genes that are upregulated in Ras CM compared to Grow CM samples with a $\log_2$ fold change > 2. (B) GSEA plots of pathways upregulated in Ras CM compared to Grow CM samples. (C) Volcano plot depicting differentially expressed genes in Ras CM samples compared to Grow CM samples. (D) qRT-PCR analysis and (E) Western blot for LCN2 expression in MCF7 cells cultured with the indicated CM. (F) qRT-PCR analysis for LCN2 expression in MCF7 cells cultured with Grow CM or conditioned media from etoposide-induced senescent IMR90T cells (Etop CM) (G) Representative images and quantification of transwell migration assay of MCF7 cells treated with the indicated CM. (H) Western blot for LCN2 expression in MCF7, SKBR3, Hs578t, BT474, MDAMB231 and T47D cells cultured with the indicated CM; G (Grow CM) and R (Ras CM). (I) Quantification of relative gap width of T47D cultures treated with the indicated CM. n = 3, ** $p < 0.01$.

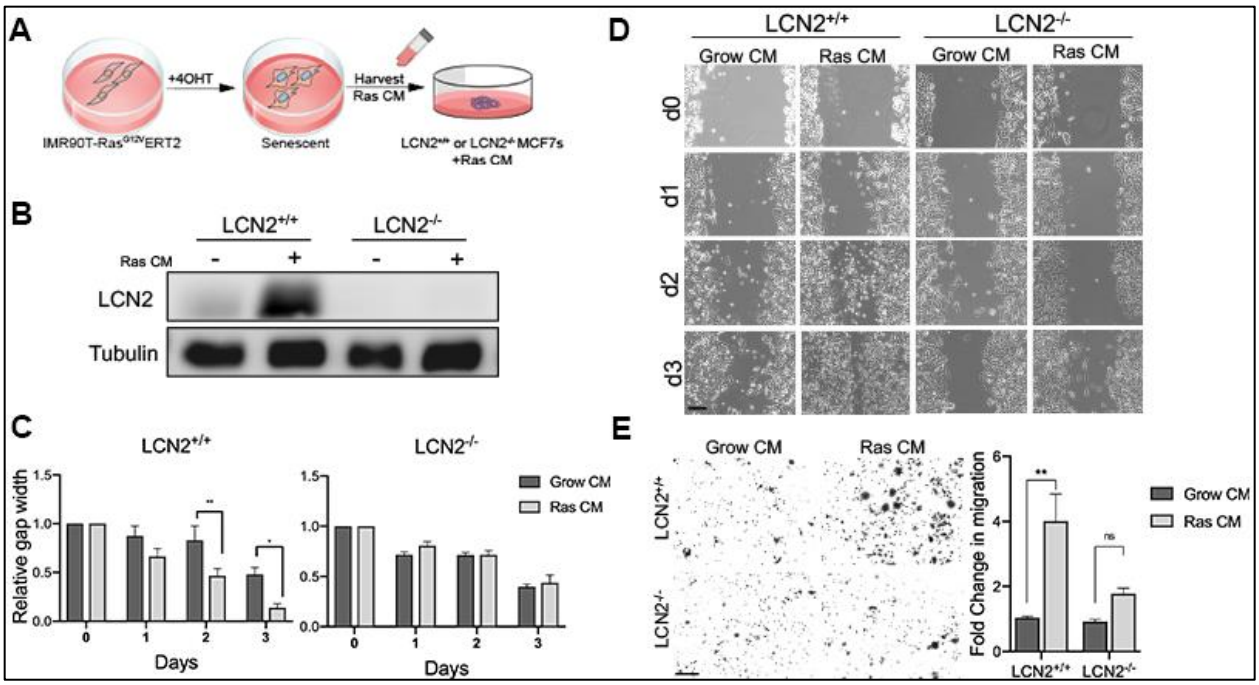

Figure 3. LCN2 upregulation is required for SASP-dependent increased migration in MCF7 cells. (A) LCN2$^{+/+}$ and LCN2$^{-/-}$ MCF7 cells were cultured with CM from either growing or senescent cells (RasCM) (B) Western blot analysis for LCN2 expression, LCN2$^{+/+}$ and LCN2$^{-/-}$ MCF7 cells cultured with the indicated CM. (C, D) Representative images of scratched LCN2$^{+/+}$ and LCN2$^{-/-}$ MCF7 cells cultured in conditioned media (CM) from growing (Grow CM) or Ras-senescent (Ras CM) IMR90T cells for 2 days. Scale bar = 200 um. (E) Representative images and quantification of transwell migration assays of LCN2$^{+/+}$ and LCN2$^{-/-}$ MCF7 cells treated with the indicated CM for 2 days. Scale bar = 200 um. n = 3, * $p < 0.05$, ** $p < 0.01$.

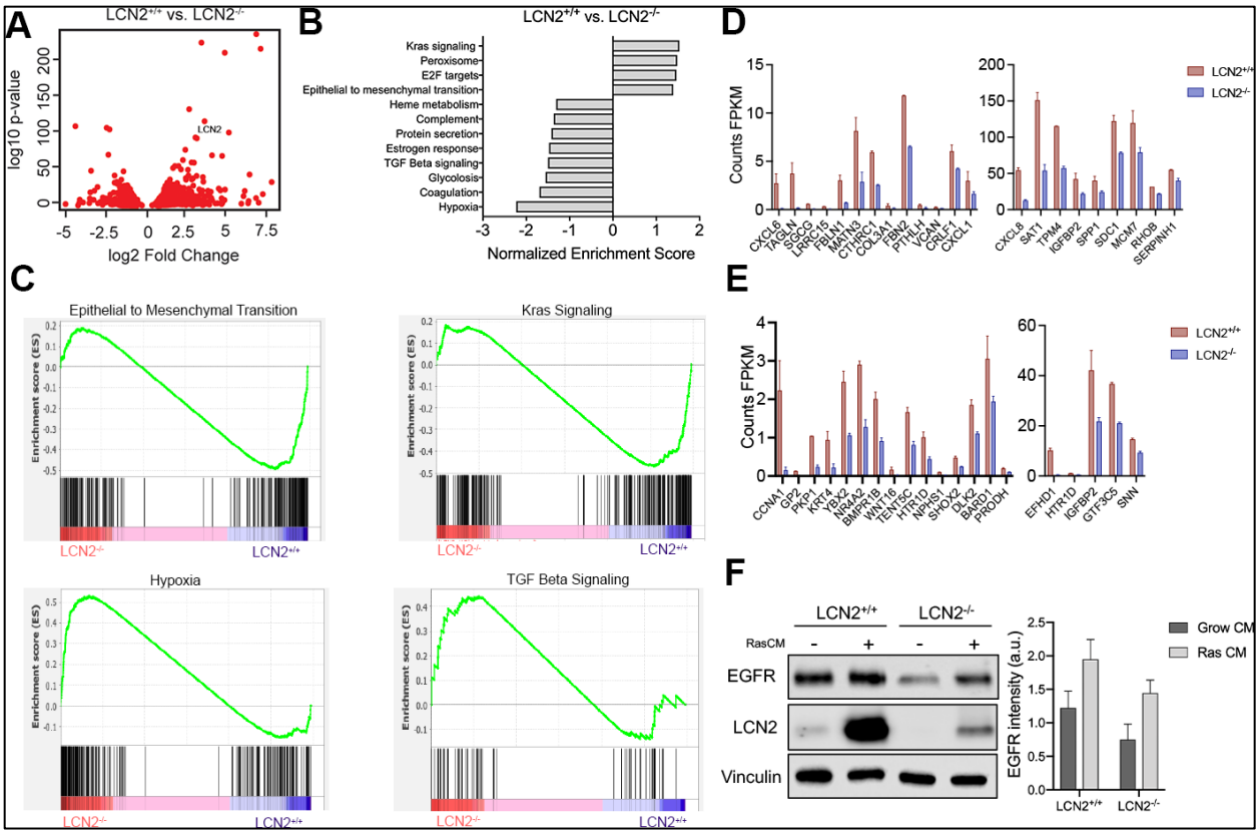

Figure 4. LCN2 potentiates the engagement of an EMT-associated expression program following exposure to senescent conditioned media. (A) Volcano plot depicting differentially expressed genes in LCN2$^{+/+}$ compared to LCN2$^{-/-}$ when treated with Ras CM. (B) Gene ontology analysis of genes that are differentially expressed in LCN2$^{+/+}$ compared to LCN2$^{-/-}$ when treated with Ras CM. (C) GSEA plots of pathways affected by LCN2 knockout when treated with Ras CM. (D) Expression level of EMT-related genes of LCN2$^{+/+}$ and LCN2$^{-/-}$ MCF7 cells when treated with Ras CM. (E) Expression level of KRas signaling-related genes of LCN2$^{+/+}$ and LCN2$^{-/-}$ MCF7 cells when treated with Ras CM. (F) Western blot analysis and quantification for LCN2 and EGFR expression in LCN2 WT or LCN2 KO MCF7 cells cultured with the indicated CM.

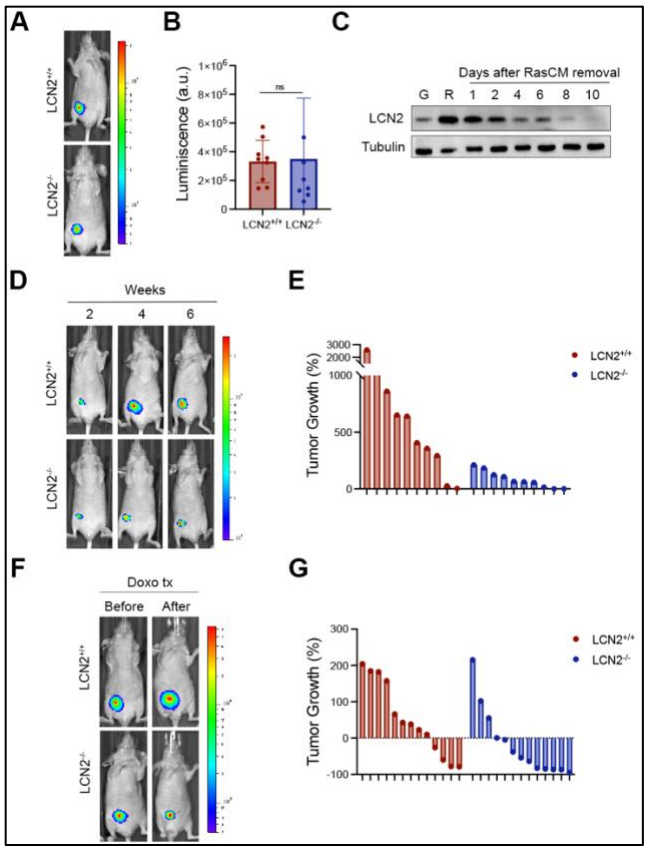

Figure 5. LCN2 expression and the SASP promote breast cancer tumor progression *in vivo*. (A) Representative images of tumor growth progression of LCN2$^{+/+}$ and LCN2$^{-/-}$ MDAMB231 GFP-Luciferase injected into mammary fat pad of nude female mice. (B) Luminescence quantification for A using a PerkinElmer IVIS Spectrum system. n = 10 (C) Western blot analysis for LCN2 expression of MDAMB231 cells after removal or RasCM, G (Grow CM) and R (Ras CM). (D) Representative images of tumor growth progression of LCN2$^{+/+}$ and LCN2$^{-/-}$ MDAMB231 GFP-Luciferase co injected into mammary fat pad of nude female mice with 1x10^{6} senescent fibroblasts. (E) Waterfall plot of the percentage change in tumor growth for LCN2$^{+/+}$ and LCN2$^{-/-}$ MDAMB231 GFP-Luciferase co injected with senescent fibroblasts. n = 10 (F) Representative images of tumor growth progression of LCN2$^{+/+}$ and LCN2$^{-/-}$ MDAMB231 GFP-Luciferase injected into mammary fat pad of nude female mice; before and 1 week after treatment with 10 mg/kg doxorubicin. (E) Waterfall plot of the percentage change in tumor growth for LCN2$^{+/+}$ and LCN2$^{-/-}$ MDAMB231 GFP-Luciferase tumors treated with doxorubicin. n = 13.

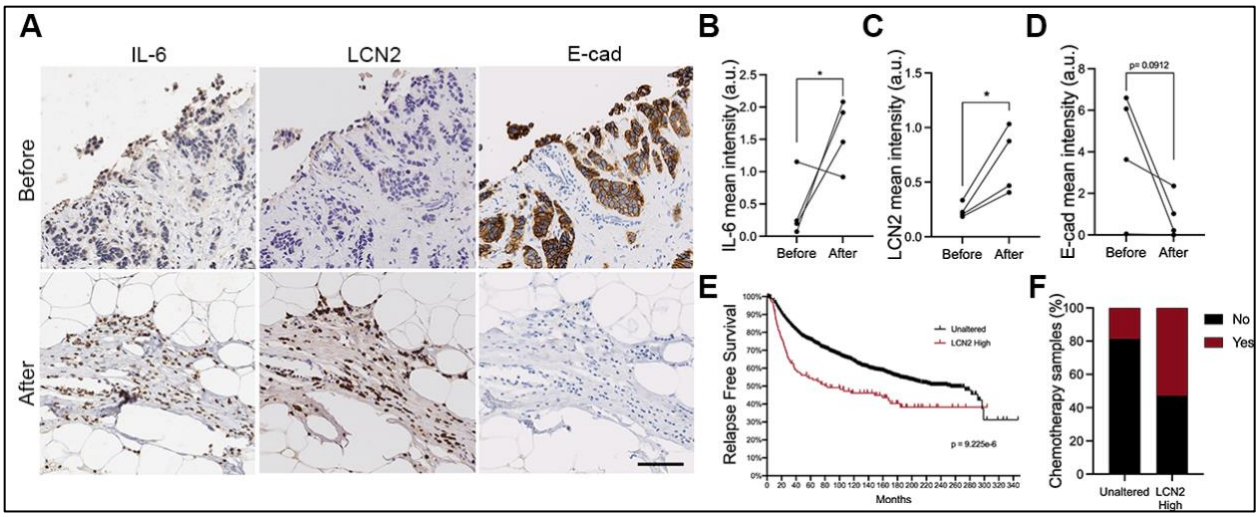

Figure 6. LCN2 upregulation following chemotherapy is a poor prognostic factor in breast cancer patients. (A) Representative images of IHC for IL-6, LCN2 and E-cad before and after neoadjuvant therapy. Scale bar = 100 um. (B) Quantification of mean intensity of IHC for IL-6 normalized by cell number per slide. (C) Quantification of mean intensity of IHC for LCN2 normalized by cell number per slide. (D) Quantification of mean intensity of IHC for E-cad normalized by cell number per slide. (E) Kaplan-Meier plots showing progression-free survival of patients with unaltered LCN2 (median, 248.95 months) and patients with high LCN2 levels (median, 83.32 months). (F) Plot showing the percentage of breast cancer patients that received chemotherapy and their LCN2 status. * $p < 0.05$.